Proceedings World Geothermal Congress 2005
Antalya, Turkey, 24-29 April 2005

Modeling of Subsidence in the Cerro Prieto Geothermal Field, B. C., Mexico

Olga Sarychikhina, Ewa Glowacka, F. Alejandro Nava Pichardo and Jose M. Romo

C I C E S E, Km. 107 Carretera Tijuana – Ensenada, 22860, Esenada, B.C., México

osarytch@cicese.mx, glowacka@cicese.mx , fnava@cicese.mx, jromo@cicese.mx

Keywords: Cerro Prieto, geothermal fields, subsidence modeling, tectonic subsidence, anthropogenic subsidence, change of the Coulomb stress.

ABSTRACT

The Cerro Prieto Geothermal Field (CPGF) is located in the Mexicali Valley, in the southern part of Salton Trough. This zone is characterized by high tectonic seismicity, heat flow and surface deformation, related with the tectonic regime of the zone. Besides the tectonic deformation, extraction of fluids in CPGF produces deformation of large magnitude (Glowacka *et al.*, 1999).

In the present work we model both natural and anthropogenic components of subsidence. We model the natural component of subsidence using known data about the seismotectonic situation and the Coulomb 2.0 program (Toda *et al.*, 1998). The resulting model shows that the subsidence due to tectonic movement constitutes approximately 4% of the observed subsidence rate.

The anthropogenic part was simulated using "tensional rectangular cracks" (Yang and Davis, 1986). Modeling was done using the Coulomb 2.0 program with a "trial and error" strategy. The resulting model for anthropogenic subsidence is based on a hydrological model of the CPGF (Halfman *et al.*, 1984; Lippmann *et al.*, 1991) and can explain the observed data with a RMS misfit of 0.79 cm/yr.

To evaluate the influence of deformation in the stress field and in the local seismicity, we calculated the change of the Coulomb stress produced by the closure of cracks in our model, as well as by tectonic movement. Our results show that the magnitude of this stress-field change, caused by extraction of fluids in CPGF, is large enough to trigger earthquakes.

1. INTRODUCTION

The Cerro Prieto geothermal field (CPGF) is located in northern Baja California, Mexico, to the south of Mexicali, in the southern portion of the Salton basin which is considered to be one of the geological provinces with the largest geothermal resources in the world (Fig. 1). Cerro Prieto is a large high-temperature (280-350°C), liquid-dominated field, contained in sedimentary rocks. The field is operated by the Mexican Federal Electricity Commission (Comisión Federal de Electricidad, CFE). Fluid extraction for electricity production began in 1973 at 1500 - 3000 m depths. Currently, the CPGF is the world's second largest geothermal field with a 720 MW capacity. Reinjection of residual water began in 1989, and currently about 20% of the extracted fluid is being reinjected at 500 - 2600 m depth.

The CPGF is located within an extremely active tectonic region, in the boundary between the Pacific and North American plate, which consists of a wide zone of transform faults from the San Andreas system with relative interplate motion of 4.9 cm/yr (Bennett *et al.*, 1996). The CPGF lies in a tectonic pull-apart basin located between two major right-lateral, strike-slip faults, the Imperial and Cerro Prieto faults.

It is well documented that ground surface deformation may accompany geothermal fluid production (Narasimhan and Goyal, 1984). Probably the best known example is Wairakei Field in New Zealand, where the maximum total subsidence reached 14 m in 1998 (Allis *et al.*, 1998).

At the CPGF, first–order leveling (Glowacka *et al.*, 1997; Glowacka *et al.*, 1999), precision gravity (Grannell *et al.*, 1979), seismological (Fabriol and Munguía, 1997) and interferometric synthetic aperture radar (InSAR) monitoring (Carnec and Fabriol, 1999; Hanssen, 2001) have reveled subsidence and triggered-seismicity, both due to fluid extraction coupled with the specific tectonic context of the zone.

The present work aims to model both the tectonic and the anthropogenic parts of the observed subsidence, and to evaluate the stress changes caused by the anthropogenic component as well as compare them with stress changes caused by the tectonic motion.

2. DATA

We use the leveling data published in Glowacka *et al.* (1999). The data were recorded during the 1994-1997 period by CFE (Lira and Arellano, 1997) and CICESE (Glowacka *et al.*, 1999). The reference point for the measurements is located in the SE part of the area, in the Cucapah mountains, and is assumed to be stable. The subsidence rate is shown in Fig. 2 (a). The dominant feature is the elliptical area with the highest subsidence rate, oriented NE-SW. This area agrees with the boundary of the geothermal anomaly. The maximum subsidence rate of ~12 cm/yr is located at the center of the extraction zone; while another, local, maximum with a subsidence rate ~9cm/yr is located to the NE of the field. The second maximum was interpreted as a fluid recharging area of the geothermal field (Glowacka *et al.*, 1999).

An estimate of the subsidence rate uncertainty was done using the approach published in Dzurisin *et al.* (2002). The estimation includes two components: the leveling error, which depends on the distance between stations, and the error due to base instability. We obtain a subsidence rate uncertainty of 0.34 cm/yr.

3. TECTONIC SUBSIDENCE MODELING

The CPGF is located between the Imperial and Cerro Prieto faults, two major strike-slip, right-lateral, step-over to the right faults, then these structures are probably responsible for natural subsidence in the studied area because they create a pull-apart zone (Fig. 1 a). Since there were no subsidence measurements before extraction began, the only way to estimate the tectonic subsidence is by modeling. We

evaluate the vertical deformation caused by the right-lateral motion between the North America and Pacific plates. We consider horizontal displacements of 3.5 cm/yr for the Imperial fault and 4.2 cm/yr for the Cerro Prieto fault (Bennett *et al*., 1996). We used the mean value of displacement velocity as an approximation of long term effect of shearing and pulling in the pull-apart center, or as evaluation of a maximum tectonic displacement during period 1994-1997, taking into account that there were not large earthquakes during this time (Sarychikhina, 2003).

Since earthquakes in the study area occur within the top 15 km (Glowacka *et al*, 1999; Rebollar *et al*, 2003), we assumed that the Imperial and Cerro Prieto faults extend from the surface to this depth, and that the upper crust is elastic. The focal mechanisms of earthquakes with M > 5 show that these faults are vertical with right-lateral motion (Frez and González, 1991). In order to locate the northern tip of the Cerro Prieto fault, and the southern tip of the Imperial fault, we used the data from González *et al*. (1998) and GPS field measurements. The possible error from supposing straight fault traces is insignificant and does not affect the final results. To calculate the subsidence we used the Coulomb 2.0 program (King *et al.*, 1994, Toda *et el*, 1998).

The tectonic subsidence rate relative to the reference point is shown in Figure 2 b. The maximum subsidence rate (0.45 cm/yr) coincides with the CPGF area, while the northeastern anomaly coincides with the previously defined recharging area. According to our results, tectonic subsidence accounts for only ~4% of the total observed subsidence.

We did not take into account the compaction and isostasy effects that can influence the modeled subsidence rate. We estimate, from published works on compaction (Carillo, 2003) and isostasy (Contreras *et al*., 1997; García Abdeslem, 2003) that these processes together can increase the tectonic subsidence rate by at most 40% of the estimated rate. Even if this additional rate is taken into account, still the tectonic subsidence rate in CPCF is of the order of millimeters per year.

The estimated tectonic subsidence is of the order of those calculated for nearby areas using other methods: 0.16 cm/yr for Laguna Salada 20 km west of Mexicali (Contreras *et al*., 2002) and 0.55 cm/y for the Vallecito-Fish Creek basin 50 km north of Mexicali (Johnson *et al*., 1983).

As it has been concluded in Glowacka *et al*. (2003) the similarity between fig. 2a and 2b can be explain by a dominant tectonic control on the origin of geothermal field (by producing crust thinning) and on sedimentation process.

4. ANTHROPOGENIC SUBSIDENCE MODELING

We proceed to model the anthropogenic component of subsidence, subtracting the calculated tectonic component from the observed subsidence.

There are several analytical and numerical models of surface deformations produced by deformation of bodies at depth; some of which can be applied to the case of fluid extraction. We modeled the anthropogenic component of subsidence using the model of a tensional rectangular crack in an elastic half-space proposed by Yang and Davies (1986).

Modeling was done using the Coulomb 2.0 program. Three closing cracks were positioned according to a hydrologic model of the field, which consist in two highly exploited reservoirs: α and β (Halfman *et al*., 1984; Lippmann *et al.*, 1991). β reservoir is divided by normal SE deeping fault H (Fig. 2 a) in two blocks: upper block ($\beta 1$) and lower block ($\beta 2$). One small crack was located under the center of the secondary subsidence center (*s. r.* – small recharge), and a large one (*L. R.* – large recharge) was located above the reservoirs that extend under a large part of the study area, in order to produce the observed subsidence outside the CPGF (Fig. 3 a).

A comparison of anthropogenic observed versus modeled subsidence rates, is shown in Figure 3(b), and the residual is shown in Figure 3(c).

Modeling was done by trial and error, and the resulting crack parameters are shown in Table I. A comparison of anthropogenic observed versus modeled subsidence rates, is shown in Figure 3(b), and the residual is shown in Figure 3(c). Both shape and magnitude of the modeled subsidence rate are quite similar to the observed; the absolute value of the residual at most observation points is about 0.0 to 0.5 cm/yr, although some local discrepancies show as much as 2.5 cm/y (Fig. 3(c)).

The root mean square error per observation point (RMS) of this model is 0.79 cm/yr. It is possible to reduce the RMS using very small cracks to eliminate the local anomalies, but in most cases these anomalies are due to a single point and may be due to measurement errors. After parameter adjustment, to fit the observed subsidence rate, the model is in agreement with the hydrological model on which it was based.

The calculated values of the crack dimensions and their closures let us estimate the change of volume in the reservoirs (without taking cooling into account) shown in Table II. If we compare this change with the rate of net extraction (extraction minus injection), we can estimate the volume of external recharge. For 1994-1997, the average extraction rate is 1.05×10^8 ton/yr, 18% of which (1.88×10^7 ton/yr) has been reinjected. Thus, the crack-induced change of volume corresponds to only ~10% of the volume decrease expected from the extraction figures. Of this 10%, only 3 % is caused by volume decrease in the hot water reservoirs, while 7 % is due to volume decrease in the cold water reservoirs.

Reservoir volume decrease together with injection account for only 28% of the extracted volume, which means that 72% of this volume is compensated by recharge from deep aquifer defined in Pelayo *et al*. (1991), Glowacka and Nava (1996) (Fig. 1). Unfortunately, this recharge zone cannot be modeled as it is much larger than the leveling network. The recharge volume of the present work is comparable to those from recharge evaluation using a poro-elastic model (Glowacka and Nava, 1996), but contradict the supposition (Pelayo *et al*, 1991) that all extraction volume is recharged

5. STRESS CHANGES AND SEISMICITY

Deformation caused by fluid extraction in geothermal reservoirs produces stress changes that may be capable of triggering earthquakes (Segall *et al.*, 1994). As determined above, 96% of the observed subsidence at the CPGF is due to reservoir fluid extraction, and it is important to assess how much this anthropogenic activity changes the stress field and influences seismicity in the area, as compared with the stress change caused by tectonic motion.

The most commonly-used stress formulation is the static Coulomb failure stress (Stein *et al*., 1992), represented as the Coulomb failure function (CFF). The change in CFF is *CSC* (Coulomb stress change) given by

$$CSC = \Delta\sigma_s + \mu(\Delta\sigma_n + \Delta p) \quad (1)$$

where $\Delta\sigma_s$ is the change in shear stress in the direction of fault slip, $\Delta\sigma_n$ is the change in normal stress (with tension positive), Δp is the change in pore-fluid pressure, and μ is an assumed "coefficient of internal friction". Typically, $\Delta\sigma_n$ and Δp are grouped within a new "effective coefficient of friction" μ', which is meant to handle the positive correlation between increased pore pressure and tensional normal stress:

$$CSC = \Delta\sigma_s + \mu'\Delta\sigma_n \quad (2)$$

where $0 \le \mu' \le \mu$

All Coulomb stresses were calculated using the Coulomb 2.0 program and a friction coefficient $\mu' = 0.4$ (Stein *et al*., 1992); to calculate the stress change caused by interplate motion, we used the same assumptions as for calculating tectonic subsidence.

We calculate the *CSC* far 1-8 km depth range. The *CSC* caused by closure of model cracks for different fault types at 6 km is shown in Figure 4. We obtained the increase of stress for reverse faulting both above and below the reservoir, and for normal and transcurrent faulting at the margins of the studied area. These results are similar to those obtained by Segall (1989) for oil and gas fields, where he modeled ground deformation caused by extraction using a poro-elastic model.

Since we have supposed uniform slip across the fault width from surface to 15 km depth, the change in Coulomb stress caused by motion along the tectonic faults is the same over this depth range. Figure 5 shows the *CSC* for different faulting mechanisms. The maximum *CSC* occurs for normal faulting (Fig. 5b) in the area between the faults. In this area stresses are relaxed for reverse faulting (Fig. 5a) and increased for strike-slip faulting (Fig. 5c). The *CSC* maximum values are listed in Table III.

6. CONCLUSIONS

During 1994-1997, tectonic induced subsidence with a maximum value of 0.45 cm/y represents only 4% of the observed subsidence for the CPGF and the surrounding area.

The anthropogenic subsidence can be modeled using tensional rectangular cracks: two corresponding to cold aquifers and 3 corresponding to the geothermal reservoirs. The crack position agrees with the hydrological model of the field. The volume change produced by the closure of the reservoir cracks accounts for only ~3% of the extracted volume, far the cold aquifers accounts for ~ 7 %. Considering that injection is about 18% of extraction, it turns out that about 72% of the extracted volume must be compensated by water from an external aquifer larger than the study area.

An analysis of the change in Coulomb stress indicates that, in the natural state, seismicity in the area is dominated by normal and transcurrent earthquakes, a well known behavior of pull-apart basin. Under fluid extraction conditions, Coulomb stress increases by more than 0.1 bar, for all faulting types. According to Harris (1998), a Coulomb stress change of 0.1 bars can trigger an earthquake. Hence the stress change caused by extraction could trigger earthquakes of all types; this supports the possibility that same seismicity at the CPGF is related to fluid extraction, as proposed by Majer and McEvilly (1982) and Glowacka and Nava (1996).

ACKNOWLEDGMENT

The results and conclusions presented in this work are solely the author's and do not necessarily express the points of view of CFE. The authors are grateful to Ortiz Figueroa for criticism and suggestions in reviewing the manuscript.

This research was sponsored in part by CONACYT, project number 35183- T and CICESE internal founds.

REFERENCES

Allis, R. G., X. Zhan and A. Clotworthy: Predicting Future Subsidence at Wairakei Field, New Zealand, *Geothermal Resources Council Trans.*, **22**, (1998), 43 – 47.

Bennett, R.A., W. Rodi and R. E. Reilinger: Global Positioning System Constrains on Fault Slip Rates in Southern California and Northern Baja, Mexico, *Journal of Geophys. Res.*, **10**, (1996), 21943 – 21960.

Carillo, R. M.: Palinoestratigrafia del neogeno en la cuenca Macuspana, Tabasco, México, *Tesis de Maestría*, CICESE, México (2003).

Carnec, C. and H. Fabriol: Monitoring and modeling land subsidence at the Cerro Prieto geothermal field, Baja California, Mexico, using SAR interferometry, *Geophysical Research Letters*, **26**, **9**, (1999), 1211 – 1214.

Contreras, J., Ch. H. Scholz and G. C. P. King: A model of Rift Basin Evolution constrained by First-order stratigraphic observation, *Journal of Geophysical Research*, **102**, **B4**, (1997), 7673 - 7690.

Contreras, J., A. Martin-Barajas and J. C. Herguera: Subsidence and Extensión Rates of Laguna Salada Basin, Northeastern Baja California, Mexico, *Eos Trans*. AGU, 83 (47), Fall. Meet. Supll., Abstract T52C – 1223, San Francisco (2002).

Dzurisin, D., M. P. Poland and R. Burgmann: Steady subsidence of Medicine Lake volcano, northern California, revealed by repeated leveling surveys, *Journal of Geophysical Research*, **107**, **B12**, (2002), 2372, 8-1 – 8-6.

Fabriol, H. and L. Munguía: Seismic activity at the Cerro Prieto geotermal area (Mexico) from August 1994 to December 1995, and relationship with tectonics and fluid exploitation, *Geophysical Research Letters*, **24**, **14**, (1997), 1807 – 1810.

Frez, J. and J. J. González: Crustal Structure and Seismotectonics of Northern Baja California. In AAPG Memoir # 47, *The Gulf and Peninsular Province of the Californias* (eds. B. Simoneit and J. P. Dauphin), (1991), 261 -283.

Garcia Abdeslem, J.: 3-D numerical Model of the Flexural Isostatic Response to Extension Induced by Crustal Scale Listric Normal Faulting, *Geofísica Internacional*, **42**, **1**, (2003), 41 – 51.

Glowacka, E., O. Sarychikhina and J. Contreras: Subsidence in the Cerro Prieto Field: Relation Between Tectonic and Anthropogenic Components, *Geothermal Resources Council Transactions*, **27**, (2003), 473 – 475.

Glowacka, E., J. J. Gonzalez and H. Fabriol: Recent Vertical deformation in Mexicali Valley and its Relationship with Tectonics, Seismicity and Fluid Operation in the Cerro Prieto Geothermal Field, *Pure and Applied Geophysics*, **156**, (1999), 591 - 614.

Glowacka, E., H. Fabriol, L. Munguía and J. J. Gonzalez: Seismicity and surface deformation around the Cerro Prieto Geothermal Field, In: *Rockbursts and Seismicity in mine* (ed. Gibowicz Lasocki), Balkema, Rotterdam, (1997), 397 – 401.

Glowacka, E. and F. A. Nava: Major Earthquakes in Mexicali Valley, México, and Fluid Extraction at Cerro Prieto Geothermal Field, *Bulletin of the Seismological Society of America*, **86**, **1A**, (1996), 93 - 105.

González, J. J., E. Glowacka, F. Suárez, G. Quiñónez, M. Guzmán, J. M. Castro, F. Riviera, and M. G. Felix, 1998, Movimiento reciente de la falla Imperial, Mexicali, B. C., *Divulgare, Ciencia para todos*, Mexicali, B. C, **6**, **22**, (1998), 4 - 15.

Granell, R. B., D. W. Tarman, R. C. Clover, R. M. Leggewie, P. S. Aronstam, R. C. Kroll and J. Eppink: Precision gravity studies at Cerro Prieto, *Proceedings*, Second Symposium on the Cerro Prieto Geothermal Field, Baja California, Mexico, Lawrence Berkeley Laboratory, Berkeley, California (1979), 329 – 331.

Halfman, S. E., M. J. Lippmann, R. Zelwer and J. H. Howard: A geologic interpretation of the geothermal fluid movement in Cerro Prieto field, Baja California, Mexico, *Assoc. Pet. Geological Bulletin*, **68**, (1984), 18 -30.

Hanssen, R. F.: Radar Interferometry, Kluwer Academic Publisher, Netherlands (2001).

Harris, R. A.: Introduction to special section: Stress triggers, stress shadows, and implications for seismic hazard, *Journal of Geophysical Research*, **103**, **B10**, (1998), 24,347 – 24,358.

Johnson, N. M., C. B. Officer, N. D. Opdyke, G. D. Woodard, P. K. Zeitler, and E. H. Lindsay: Rates of late Cenozoic Tectonism in the Vallecito – Fish Creek basin, *Geology*, **11**, (1983), 664 – 667.

King, G. C. P., R. S. Stein, and J. Lin: Static Stress Changes and the Triggering of Earthquakes, *Bulletin of the Seismological Society of America*, **84**, **3**, (1994), 935 – 953.

Lippmann, M. J., A. H. Truesdell, A. M. Mañón and S. E. Halfman: A review of the hydrogeologic-geochemical model for Cerro Prieto, *Geothermics*, **20**, (1991), 39 – 52.

Lira, H. and J. F. Arellano: Resultados de la nivelación de precisión realizada en 1997, en el campo geotérmico Cerro Prieto, *Informe técnico RE 07/97*, CFE, México (1997).

Majer, E. L. and T.V. McEvilly: Seismological studies at the Cerro Prieto Geothermal Field, 1978-1982, *Proceedings*, Fourth Symposium on the Cerro Prieto Geothermal Field, Baja California, Mexico, Comisión Federal de Electricidad, (1982), 145 – 151.

Narasimhan, T. N. and K. P. Goyal: Subsidence due to geothermal fluid withdrawal, in Man – Induced Land Subsidence", En: T. L. Holzer (ed.), *Reviews in Engineering Geology*, **6**, Geol. Soc. Am., Boulder, Colo, (1984), 35 – 66.

Pelayo, A., A. Razo, L. C. Gutiérrez, F. Arellano, J. M. Espinoza and J. L. Quijano: Main geothermal field of Mexico; Cerro Prieto geothermal field, Baja California, The Geology of North America, ed. Salas G. P. , P-3, *Economic Geology*, Mexico, GSA, (1991), 23 – 57.

Rebollar, C. J., L. M. Reyes, L. Quintanar and J. F. Arellano: Stress Heterogeneity in the Cerro Prieto Geothermal Field, Baja California, Mexico, *Bulletin of the Seismological Society of America*, **93**, **2**, (2003), 1 – 22.

Sarychikhina, O.: Modelación de subsidencia en el campo geotérmico Cerro Prieto, *Tesis de Maestría*, CICESE, México (2003).

Segall, P.: Earthquakes triggered by fluid extraction, *Geology*, **139**, (1989), 535 – 560.

Segall, P., J-R. Grasso and A. Mossop; Poroelastic stressing and induced seismicity near the Lacq gas field, southwestern France, *Journal of Geophysical Research*, **99**, **B8**, (1994), 15,423 – 15,438.

Stein, R. S., G. C. P. King and J. Lin: Change in failure stress on the southern San Andreas fault system caused by the 1992 Magnitude=7.4 Landers earthquake, *Science*, **258**, (1992), 1328 – 1332.

Toda, S., R. S. Stein, P. A. Reasenberg and J. H. Dieterich: Stress transferred by the Mw=6.9 Kobe, Japan, shock: Effect on aftershocks and future earthquake probabilities, *Journal of Geophysical Research*, **103**, (1998), 24543 – 24565.

Yang, X. and P. M. Davis: Deformation due to a rectangular tensional crack in an elastic half-space, *Bulletin of the Seismological Society of America*, **76**, **3**, (1986), 865 – 881.

Table I: Model cracks parameters.

Crack	Parameters							
	Center (m)			(m)			(°)	
	x	y	z	p	c1	c	azm	ang
α	664032	3584530	1100	-0.05	3471	2019	140	1
β_1	666667	3586700	2100	-0.10	1099	2144	138	4
β_2	669000	3586000	2250	-0.12	737	2293	138	4
s. r.	673352	3590150	1500	-0.08	2907	2333	142	7
L. R.	669057	3587291	996	-0.04	5806	6347	139	1

x, y, z (center of crack), p (crack closure), c and c1 (crack dimensions), and azm (azimuth) and ang (dip) (crack orientation)

Table II: Volume change caused by model cracks closure.

Crack	Volume change (m^3)	
α	1.4×10^6	3.2×10^6
β_1	1×10^6	
β_2	0.8×10^6	
s. r.	2.1×10^6	8.1×10^6
L. R.	6×10^6	
Total	$\mathbf{1.1\times10^7}$	

Table III: Coulomb Stress Change (bars).

Fault mechanism	Tectonic faults		Model cracks	
	minima	maxima	minima	maxima
Strike-Slip	-3.2	3.6	-0.2*	0.3*
Normal	-0.3	4.0	-1.0*	0.4*
Reverse	-1.1	1.1	-0.4*	1.7*

* - *CSC* at depth of 6 km

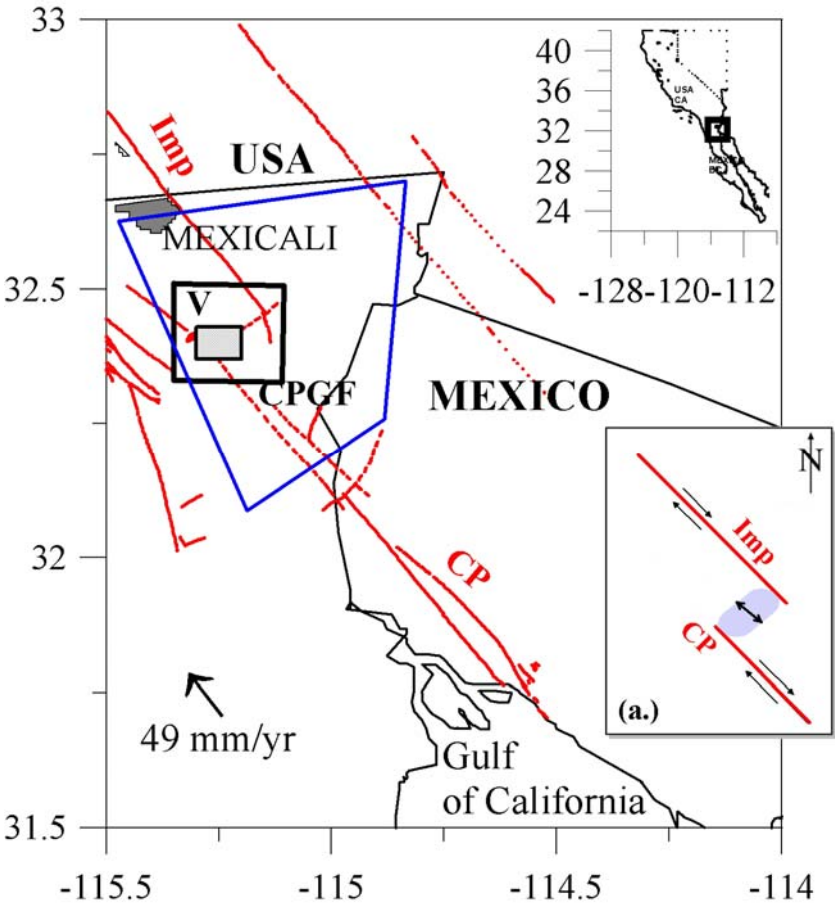

Figure 1: Location map. CPGF - Cerro Prieto Geothermal Field (small rectangle), Large rectangle - study area, Imp - Imperial fault, CP - Cerro Prieto fault, V - Cerro Prieto volcano, blue polygon - deep aquifer area. (a) Schematic presentation of the pull-apart basin. (Modified from Glowacka *et al*., 2003).

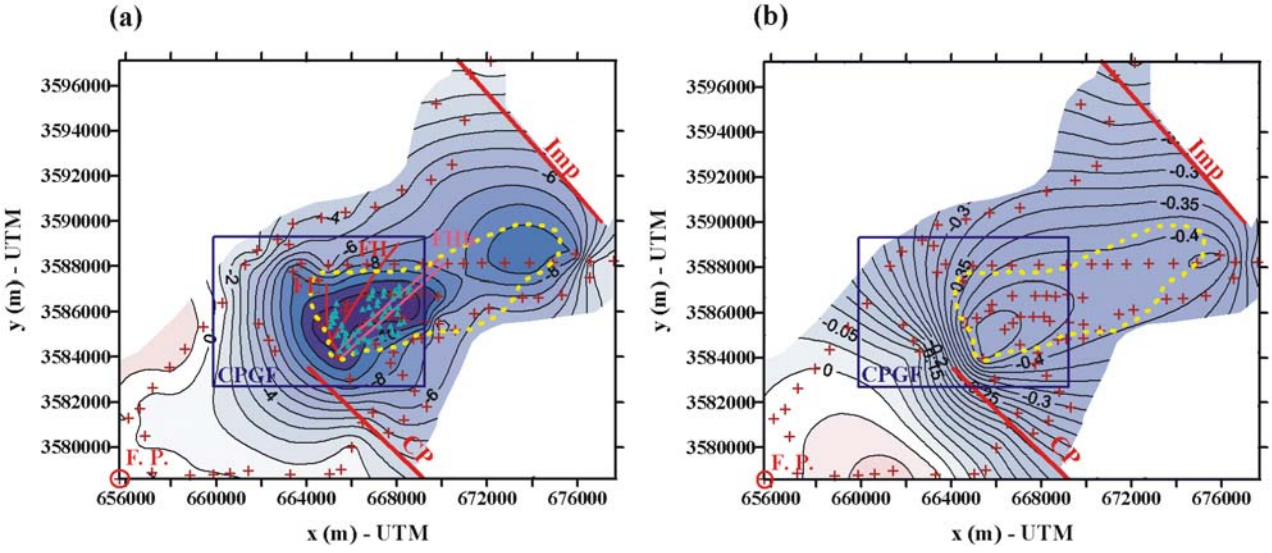

Figure 2: (a) Observed subsidence rate (1994 - 1997) in cm/yr. Light blue triangles ─ extraction wells. Rectangle ─ CPGF. Dotted yellow line ─ T ≥ 300° isotherm. Brown crosses ─ leveling points. F. P. ─ fixed point. FH ─ surface projection of H fault, FHb ─ intersection of H fault with the top of the β reservoir, FL ─ L fault. (b) Tectonic subsidence rate relative to the fixed point in cm/yr. (Modified from Glowacka *et al*., 2003).

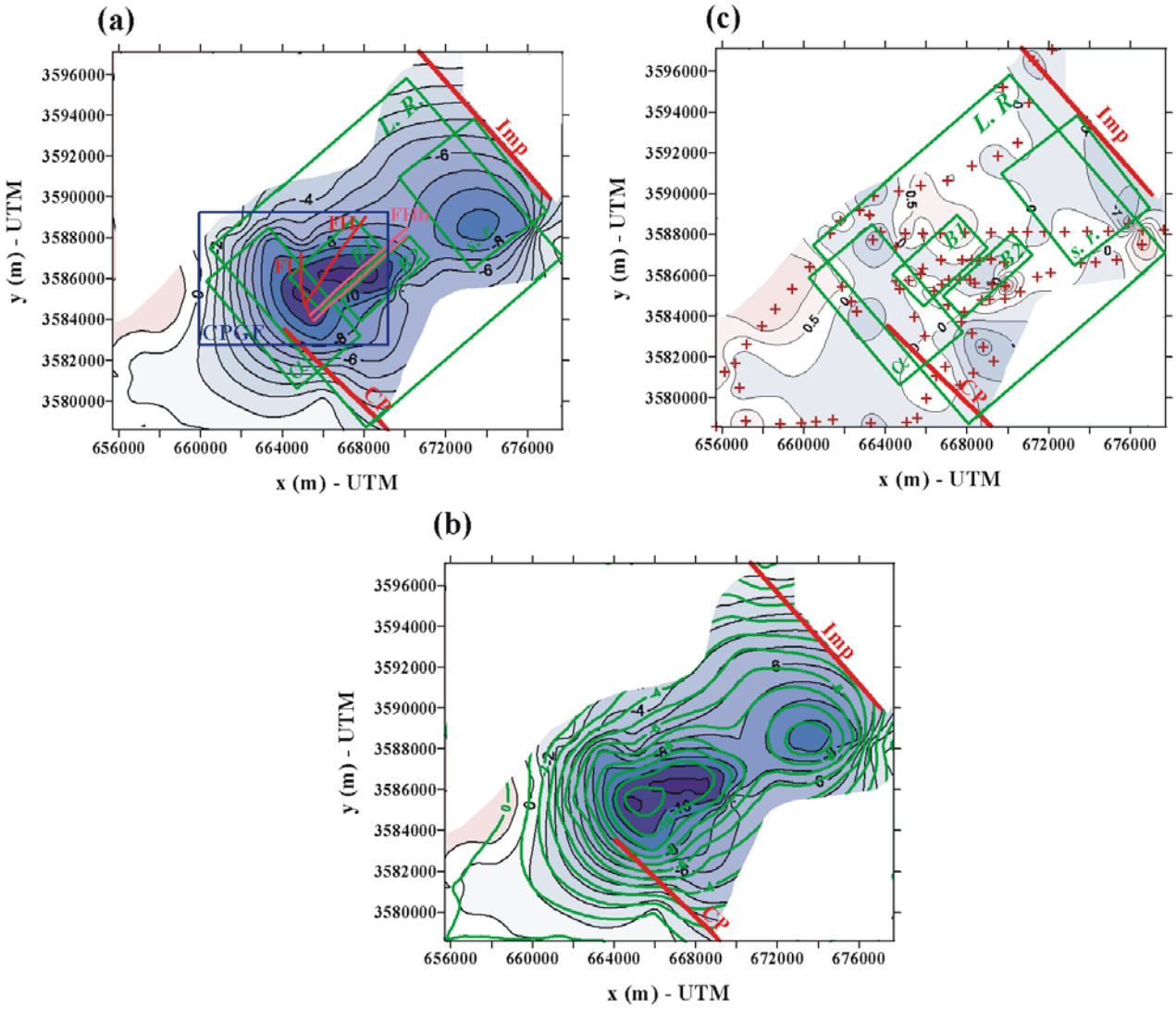

Figure 3: Modeling of anthropogenic subsidence. (a) Surface projection of cracks. Isolines are observed subsidence rate (minus tectonic component). (b) Comparison of observed (black) to modeled (green) subsidence rates. (c) Residual (cm/yr).

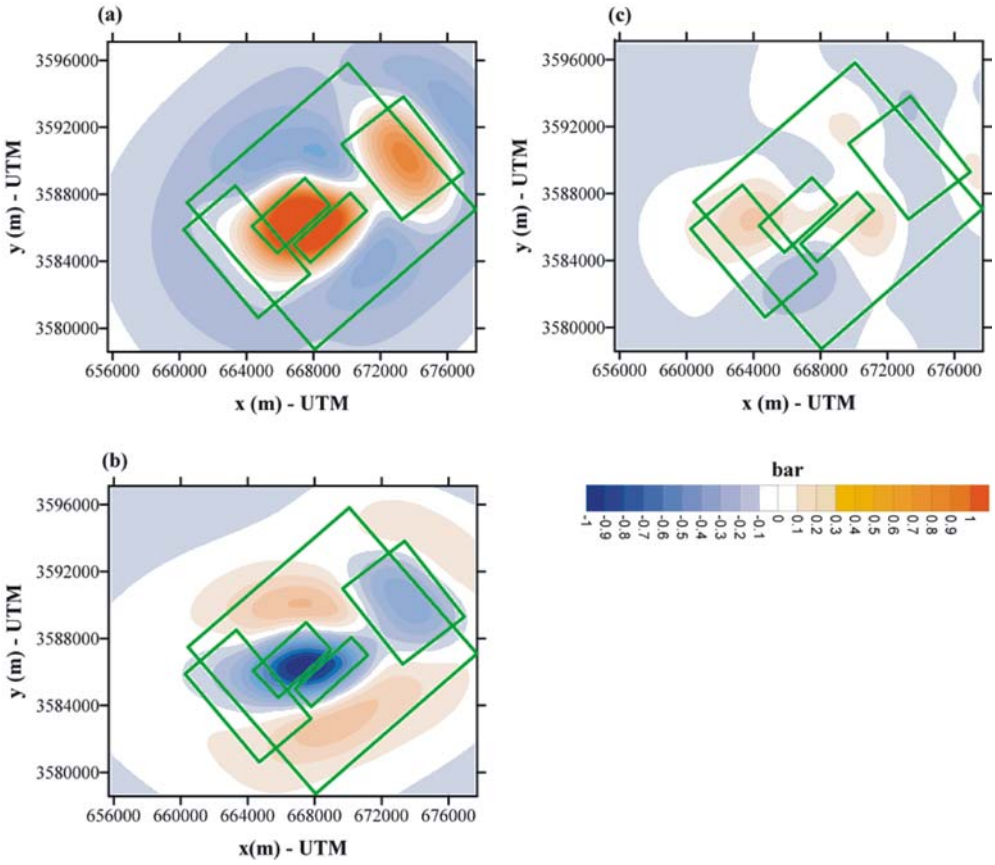

Figure 4: Coulomb stress change at 6 km depth caused by closure of cracks model for (a) ─ Reverse, (b) ─ Normal, (c) ─ Strike-Slip fault mechanism

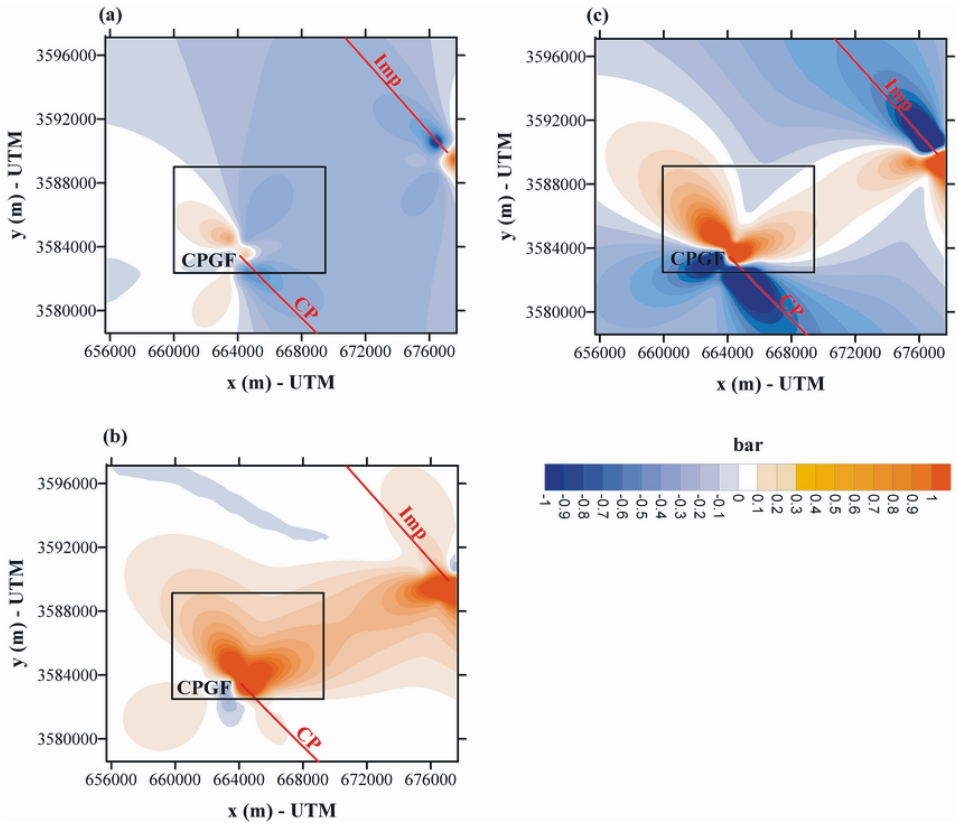

Figure 5: Coulomb stress change caused by slip along the Imperial and Cerro Prieto faults for (a) ─ Reverse, (b) ─ Normal, (c) ─ Strike-Slip fault mechanism.